Surface Structure Analysis of X12CrNiMoV12-3 and X6CrNiTi18-10 Steel Samples Processed by Laser Shot Peening (LSP)

David Bricín[1,2*], *Hynek* Gilík[2]

[1]Centrum výzkumu Rez s.r.o., Morseova 1245/6, 301 00, Pilsen, Czech Republic
[2]Department of Material Science and Technology, University of West Bohemia, Univerzitni 8, 301 00 Pilsen, Czech Republic

Abstract. The aim of the experiment was to verify the influence of the chosen strategy of laser shot peening (LSP) on the structure and surface properties of samples made of martensitic steel X12CrNiMo12 and austenitic steel X6CrNiTi18-10. The analyses performed consisted of surface topography analysis of the samples, using a confocal microscope, Olympus LEX|T OLS 5000 and metallographic analysis using a Carl Zeiss Observer Z1m light microscope and a Tescan Mira 3 scanning electron microscope. The metallographic analysis was complemented by the measurement of microhardness HV0.01, which was performed using a Struers DuraScan semi-automatic hardness tester. The LSP process introduced plastic deformation into the surface layer of both materials analysed. The plasma and shock wave generated during the process further affected the surface roughness of both tested materials, which was reflected by an increase in the value of the roughness parameter Rz. Microhardness measurements showed that the influence of the LSP process can increase the surface hardness of the material. Metallographic analysis using light microscopy methods failed to identify differences between the structure near the shot peened surface and the non-peened surface, probably due to the coarse grain structure of both materials analysed.

1 Introduction

Laser Shot Peening (LSP) technology is one of the surface treatments of materials that significantly harden their surface layer, thereby reducing their susceptibility to failure by initiating cracks from their surface [1-2]. This makes the technology applicable to the most exposed areas of dynamically and statically stressed machine components, such as turbine blade parts or welded joints [3]. The technology works on the principle of the interaction of a pulsed laser beam with the surface of the material to form a high-pressure plasma [3-4]. When plasma is generated, heat and shock waves are generated and propagate into the material being shot and its surroundings. The heat generated in this process, however, can reduce the effect of the LSP process. For this reason, a thin ablative layer in the form of, for

* Corresponding author: david.bricin@cvrez.cz, bricda@kmm.zcu.cz

example, black adhesive tape is applied to the surface of the material to be shot to protect the surface of the material to be shot against thermal effects. In addition to the ablative tape, a stream of water, the so-called cover layer, flows over the surface of the material to be shot. This uniform layer is designed to trap the emerging plasma and thus increase the time for which the emerging plasma acts on the surface of the material, see Fig. 1. In addition to the above, the type of laser beam used and its wavelength, the size of the beam spot, the pulse frequency, the pulse overlap, the firing strategy, and the properties and type of the material to be shot also affect the results achieved when shooting the material surface using the LSP method [3, 5]. Thus, the aim of this paper was to verify the ability of the selected laser pulse shooting strategy, to achieve the desired surface hardening of two types of steels, namely steel with austenitic structure X6CrNiTi18-10 and steel with martensitic structure X12CrNiMoV12-3, which are used for components in the energy industry such as turbine blades and piping systems.

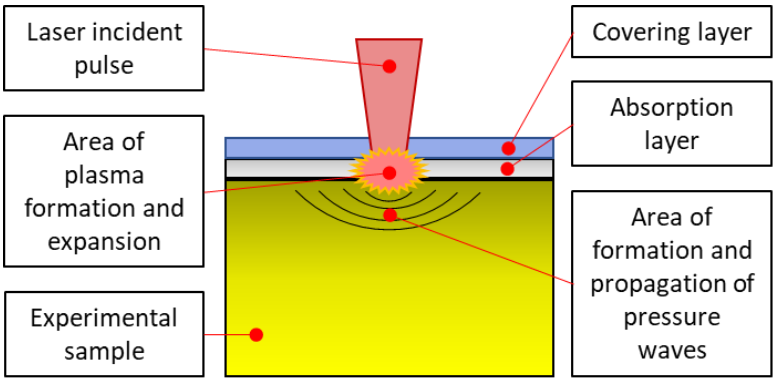

Fig. 1. The principle of the LSP process. When the laser strikes, the absorber layer is vaporized. A plasma is formed between the sample and the cover layer, flowing water, which creates a shock pressure wave propagating into the sample material volume

2 Experimental materials and methods

Two types of material were selected for the experiment, namely the austenitic refractory chromium-nickel steel stabilized with titanium X6CrNiTi18-10 and chromium-nickel-manganese-vanadium steel X12CrNiMoV12-3. Their chemical composition, recorded by EDS analysis, is given below, see Tab. 1. The initial microstructure of the samples taken is then shown in the metallographic images, see Figs. 2-3. The first of these materials, X6CrNiTi18-10 steel, is commonly used for the manufacture of piping systems. The second material, X12CrNiMoV12-3 steel, is commonly used for the manufacture of steam turbine blades.

Table 1. Chemical composition of analysed materials

Element/material	**Fe [hm.%]**	**Si [hm.%]**	**Mn [hm.%]**	**Cr [hm.%]**	**Mo [hm.%]**	**Ni [hm.%]**	**V [hm.%]**	**Ti [hm.%]**
X6CrNiTi18-10	68.4±0.13	0.6±0.0	1.9±0.0	18.7±0.1	-	10.1±0.13	-	0.3±0.0
X12CrNiMoV12-3	81.5±0.3	0.2±0.0	0.8±0.0	12.6±0.1	2±0.1	2.7±0.16	0.3±0.0	-

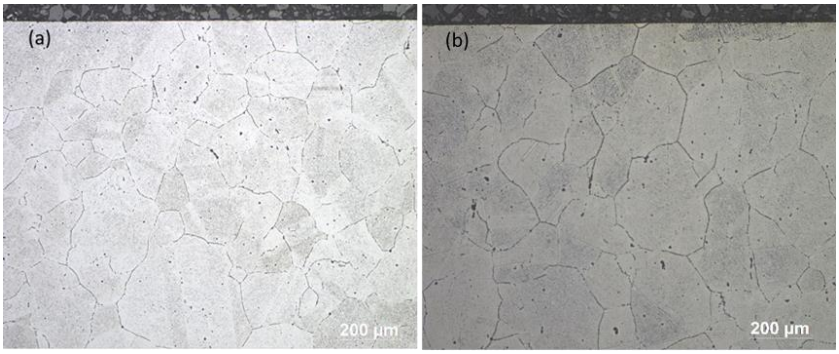

Fig. 2. Microstructure of X6CrNiTi18-10 steel samples. (a) section in the direction of firing; (b) section in the direction perpendicular to the direction of firing

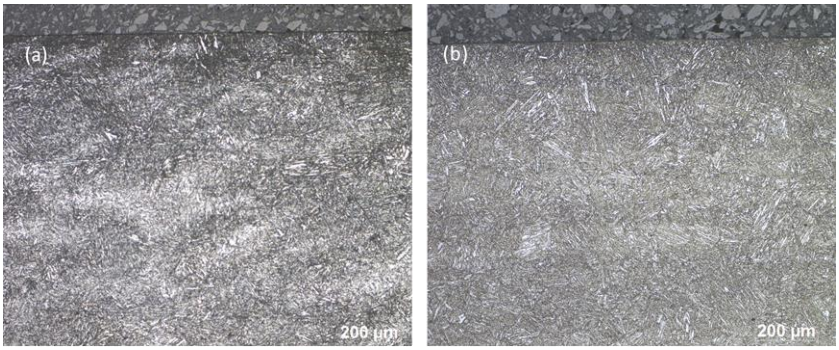

Fig. 3. Microstructure of X12CrNiMoV12-3 steel samples. (a) section in the direction of firing; (b) section in the direction perpendicular to the direction of firing

The materials for this experiment were supplied in the form of sheet metal plates with a nominal thickness of 6.5 mm for the X12CrNiMoV12-3 material and a thickness of 5.5 mm for the X6CrNiTi18-10 material. The delivered material was shot peened using a solid-state diode laser with Bivoj marking in the HiLASE centre (FZU, Dolní Břežany, CZE). This laser operates at a wavelength of 1030 nm. In this case, a pulse energy of 3 J and a duration of 30 ns for each pulse was chosen to focus on the sample surface. When shooting the surface of the delivered materials, a strategy was chosen in which the previous pulse was 52.8 % covered by the next pulse. The overlap between each pulse sequence was then 77.8%. Vinyl tape was used as a protective ablation layer. After surface shot peening of the samples, two samples were taken from each sheet of metal. The first sample was taken in the direction of the laser pulse shot sequence (longitudinal direction), the second in the direction perpendicular to it. An Olympus Lext OLS5100 confocal laser scanning microscope (Olympus Czech Group, s.r.o., Prague, CZE) was used to analyse the surface topography of the samples before and after the LSP shot process. A CarlZeiss Observer Z1m light microscope (Carl Zeiss s.r.o., Prague, CZE) and a Tescan Mira 3 scanning electron microscope (TESCAN ORSAY HOLDING, a.s., Brno, CZE) were used to analyse the differences in the microstructure of the sample surface. To induce the microstructure of the X6CrNiTi18-10 material, an etchant consisting of nitric acid (HNO_3), Hydrofluoric acid (HF) and glycerine ($C_3H_8O_3$) was used in a 2:2:1 ratio. A Vilella-Bain etchant was then used to induce the microstructure of the X12CrNiMoV12-3 material. The metallographic analysis was complemented by the measurement of the microhardness progression HV0.01, which was performed using a Struers DuraScan semi-automatic hardness tester (Struers GmbH, Roztoky u Prahy, CZE). The first indentation was performed for each sample at a distance of

50 µm from the edge of the sample. The distance between indentations was set to 50 µm. Hardness measurements were stopped in the distance where the hardness measured before the experiment was reached at the centre of each sample.

3 Experimental results and discussion

The LSP shot peening of the surface of the samples caused changes in the surface topography and roughness of the analysed samples, see Fig. 4 and Tab. 2. From the images, see Fig. 4, it can be seen that the surface of the samples was more affected by the austenitic steel, where the shot peening caused a more pronounced surface deformation, which was manifested by an increase in the variance of the values of the height profile of their surface compared to the martensitic steel samples and the surfaces of the samples that were not affected by LSP shot peening. These changes in surface topography are then reflected by the change in surface roughness of the samples after the LSP process, see Tab. 2.

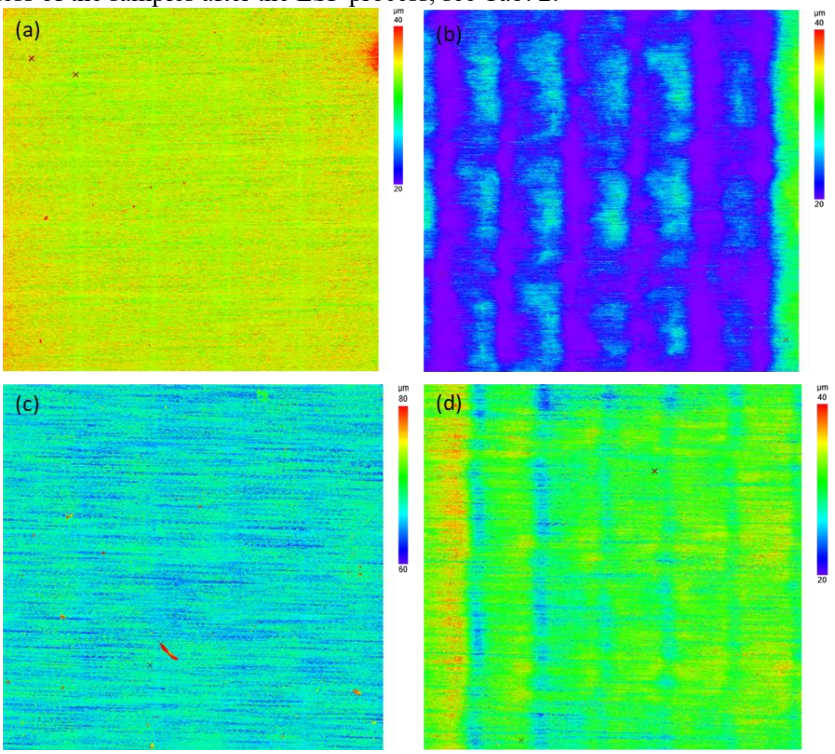

Fig. 4. (a) Height profile of the sample surface before LSP shooting, material X6CrNiTi18-10; (b) Height profile of the sample surface after LSP shooting, material X6CrNiTi18-10; (c) Height profile of the sample surface before LSP shooting, material X12CrNiMoV12-3; (d) Height profile of the sample surface after LSP shooting, material X12CrNiMoV12-3

In the case of the samples analysed, no significant change in their arithmetic mean surface roughness value Ra was observed, see Tab. 2. The fact that there was no significant change in this surface roughness parameter of the analysed samples was related to the fact that their surface was protected by ablative tape. Its use reduces the susceptibility of the sample surface material to melting and evaporation, which leads to the formation of surface craters, which can increase the surface roughness of the samples [6]. The presence of surface microcraters is more indicative of the presence of the mean depth of roughness parameter Rz. In the case of samples made of X6CrNi18-10 material, after LSP shot peening, the value of this

parameter increased by about 10 % in the longitudinal direction and by about 54% in the transverse direction. For the X12CRNiMoV12-3 samples, the value of this parameter increased by about 2 % in the longitudinal direction and by about 29 % in the transverse direction. The size and number of depressions or craters could be further influenced by the pulse energy and duration [7].

Table 2. Linear profile roughness

Material	Longitudinal direction		Transverse direction	
	Ra[µm]	Rz[µm]	Ra[µm]	Rz[µm]
X6CrNiTi18-10	1.3±0.03	13±0.84	1.2±0.05	9.5±0.57
X6CrNiTi18-10 (LSP)	1.4±0.09	14.3±1.07	2.2±0.36	14.6±1.91
X12CrNiMoV12-3	1.7±0.04	16.2±0.74	1.6±0.19	13.3±0.96
X12CrNiMoV12-3 (LSP)	1.6±0.04	16.5±0.81	1.8±0.21	17.2±2.59

The pulse energy input causes changes in the microstructure of the material and changes in the applied residual stress. These changes are then reflected in a change in the hardness of the surface layer of the samples, see Figure 5. In the case of the X6CrNiTi18-10 austenitic steel samples, the hardness measurements determined the depth of substrate influence on the sample in the shooting direction to be approximately 0.6 mm, and in the direction perpendicular to this direction to be approximately 1.2 mm. In the case of samples made of martensitic steel X12CrNiMoV12-3, the depth of influence in the shooting direction was about 0.2 mm, in the perpendicular direction about 0.4 mm.

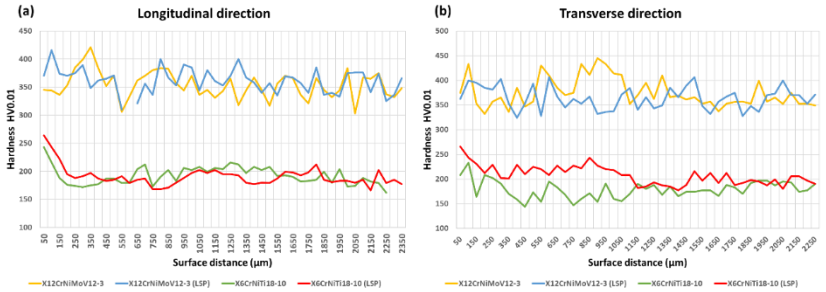

Fig. 5. Comparison of microhardness HV0.01 (a) section in the direction of firing; (b) section in the direction perpendicular to the direction of firing

It is known from the literature that the waveform of the imposed residual compressive stresses by a single shot, is uniform in the volume of the material, with a small depth gradient [8]. However, when multiple shots are taken, as shown by the simulation results in [9], a non-uniform distribution of the applied residual stresses occurs. This non-uniformity can then become apparent when measuring the microhardness of the material as in the case of this study. The highest hardness was achieved at or near the surface of the material. For austenitic steel X6CrNiTi18-10, the highest hardness value was recorded at a distance of 50 µm from the sample surface, in both directions analysed. In the shooting direction, a hardness of 264HV0.01 was measured at the surface of the sample shot by the LSP method. Compared to the unaffected sample surface, this was an increase in hardness of approximately 9 % in this region. In the direction perpendicular to the shooting direction, a hardness of 266HV0.01 was measured on the LSP-treated sample surface. Compared to the unaffected sample surface, this was an increase in hardness of approximately 28 % in this region.

For martensitic steel X12CrNiMoV12-3, the highest hardness was recorded for the specimens shot by the LSP method at a distance of 0.1 mm from the specimen surface for the cut in the direction of shooting and at a distance of 0.35 mm from the specimen surface for the perpendicular direction. In the shooting direction, 416HV0.01 hardness was measured in this area from the surface of the LSP specimen. Compared to the unaffected sample surface,

this was an increase in hardness of approximately 21 % in this region. In the direction perpendicular to the direction of firing, a hardness of 353HV0.01 was measured in this area from the LSP specimen surface. Compared to the unaffected sample surface, this was an increase in hardness of approximately 5 % in this region. The introduced energy can then affect the microstructure of the surface of the shot peened material to a large extent. See Figs. 6-7 below for the surface structure of the samples recorded using an optical microscope.

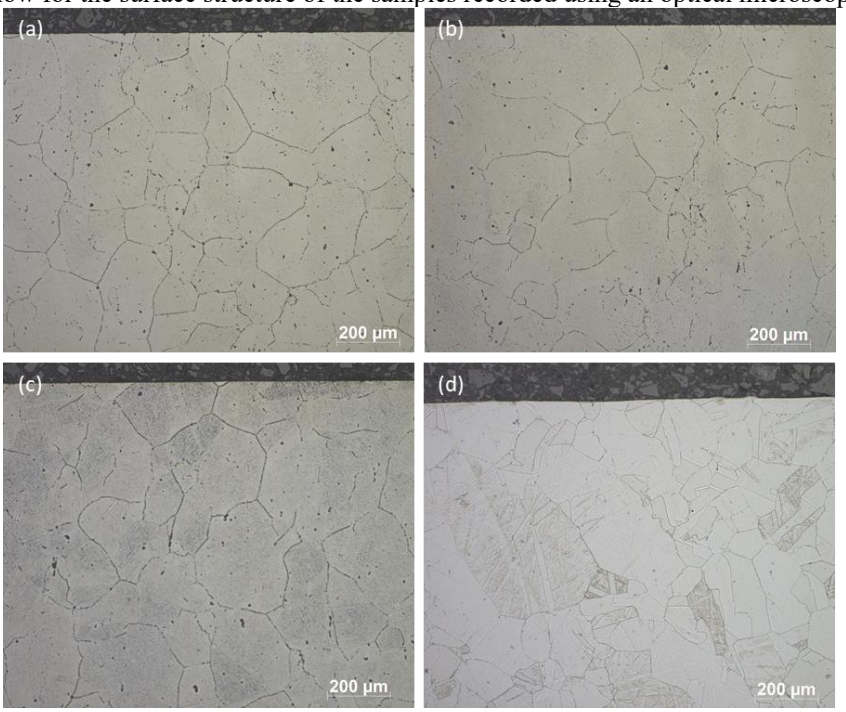

Fig. 6. Comparison of the surface structure of X6CrNiTi18-10 austenitic steel samples before and after LSP shot peening. (a) Structure of the unaffected surface, longitudinal direction- in the direction of shooting; (b) Structure of the surface after LSP shot, longitudinal direction- in the direction of shooting; (c) Structure of the unaffected surface, transverse direction- perpendicular to the direction of shooting; (d) Structure of the surface after LSP shot, transverse direction- perpendicular to the direction of shooting

From the metallographic images, taken by light microscopy (LM), it can be seen that the structure of the X6CrNiTi18-10 austenitic steel samples has not changed significantly due to the LSP process, see Fig. 6.

In a study [10], which investigated the microstructural changes in the surface of austenitic steels due to their LSP shot peening, it was found that grain refinement can occur during the LSP process, which mainly involves plastic deformation of the material surface by twinning and strain-induced martensitic transformation. However, none of the above was observed in the material structure in this case. The absence of significant microstructural changes due to the LSP process is related to the coarseness of the grains of the material used. As it was found the coarse grain structure of the material is able to absorb the generated shock wave in its volume without successfully refining the microstructure of the material [11]. This is also because in coarse-grained material there are far fewer suitably oriented planes of slip relative to the external load in which dislocations could move, and so it cannot experience such a significant increase in their density, which would result in a noticeable microstructural change, as in the case of bulk fine-grained austenitic steels.

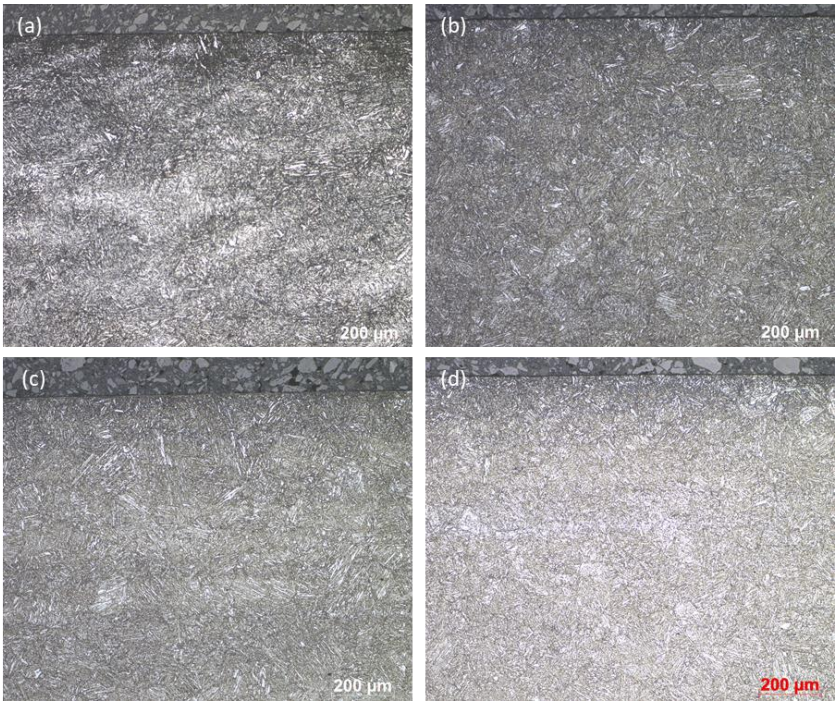

Fig. 7. Comparison of the surface structure of the martensitic steel X12CrNiMoV12-3 samples before and after LSP shot peening. (a) Structure of the unaffected surface, longitudinal direction- perpendicular to the shooting direction; (b) Structure of the surface after sniping, longitudinal direction- perpendicular to the shooting direction; (c) Structure of the unaffected surface, perpendicular direction- perpendicular to the shooting direction; (d) Structure of the surface after LSP shot peening, perpendicular direction- perpendicular to the shooting direction

Similarly, no significant structural change was captured by LM methods in the case of the shot peened surface of the martensitic steel X12CrNiMoV12-3, see Figure 7. As it has been found that shot peening of the surface of martensitic steels by LSP can lead to refinement of the martensite laths, reduction in the size of the original carbides and precipitation of nano-carbides in their surface [12-13]. However, these differences cannot be observed by LM methods.

Below are metallographic images that were obtained by analysing the structure of the shot peened samples using an electron backscatter detector (EBSD), see Figures 8-9. Figures 8(a) and 9(a) show the reconstructed grain boundaries of the two analysed materials. From the image, see Figure 8(a), it can be seen that some of the grains of the austenitic steel X6CrNiTi18-10 bear traces of plastic deformation by twinning. As noted, see ref. [10], this phenomenon can occur in the case of surface shooting of the following types of material. In the structure of the martensitic steel X12CrNiMoV12-3, the described refinement of the martensite lath structure was not observed, see Fig. 9(a), as in the case of the previously cited study, and see Ref. [12]. This is due to the fact that at such low magnification these structures are beyond the resolution of the method used. Figures 8(b) and 9(b) then show ipf maps of the surface structure of the analysed materials. The results show that the grain orientation is coincidental for both analysed materials. Therefore, the LSP process did not cause significant changes in their orientation. Using a component designed to determine the fraction of recrystallized structure, it was possible to observe the depth of plastic deformation in the surface structure of the X6CrNiTi18-10 austenitic steel samples, see Figure 8(c). The depth of this plastic deformation was not uniform over the entire surface. Its value reached values

of units to tens of micrometres. In the case of the X12CrNiMoV12-3 martensitic steel samples, this area could not be visualized, probably because of the low resolution of the method, at the low magnification used. The last images document the microstructure of the samples when the component is used to show areas where significant plastic deformation of the material structure has occurred, see Figure 8(d) and Figure 9(c). From figure 9(c), it can again be seen that any changes in the structure of the X12CrNiMoV12-3 martensitic steel are below the resolution of this method at its low magnification. For the austenitic steel samples, see Fig. 8(d), it can be seen that, in addition to plastic deformation in the surface layer, traces of the metallographic preparation operations have become visible.

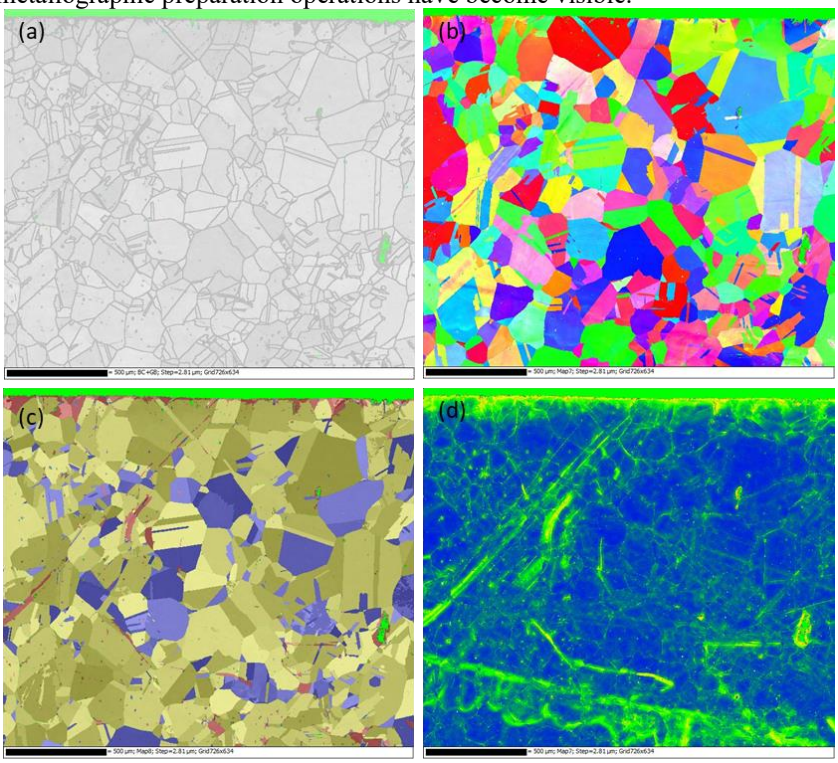

Fig. 8. (a) reconstruction of grain boundaries; (b) ipf map of the surface; (c) recrystallized fraction map, red colour shows plastically deformed grains, blue colour shows recrystallized grains; (d) local misorientation map shows areas with significant plastic deformation.

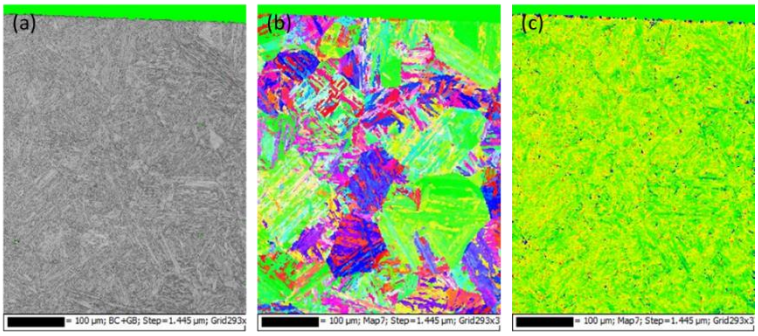

Fig. 9. (a) reconstruction of grain boundaries; (b) ipf map of the surface; (c) local misorientation map shows areas with significant plastic deformation

4 Conclusion

The aim of the study was to verify the quality of surface hardening of two types of steels, namely austenitic steel X6CrNiTi18-10 and martensitic steel X12CrNiMoV12-3 whose surface was shot peened by LSP. The results of the performed experiment confirmed that the surface layer of the substrate was influenced by its shot peening in the case of both analysed materials. The results obtained are summarized below:

- The more significant influence on the surface of the material occurred in the case of austenitic steel X6CrNiTi18-10. In this steel, a more pronounced plastic deformation occurred in the surface layer, which was manifested by a greater depth of the height profile.
- For both materials analysed, the value of the linear parameter of the mean depth of roughness Rz increased in both directions.
- Material hardness measurements showed an increase in surface hardness for both materials analysed. Higher depth of influence was achieved for austenitic steel X6CrNiTi18-10. The depth of influence on the surface of the material then varied for each measurement direction.
- The analysis of the structure of the samples by LM methods did not reveal any obvious differences between the LSP shot peened surface and the unshot peened surface for both the austenitic steel X6CrNiTi18-10 and the martensitic steel X12CrNiMoV12-3.
- EBSD analysis showed non-uniform plastic deformation in the surface layer of the X6CrNiTi18-10 austenitic steel samples to a depth of tens of micrometres. Other significant microstructural changes were not observed at the magnification used due to the low resolution of the method at this magnification.
- No significant change in the structure of the X12CrNiMoV12-3 martensitic steel samples was observed at the magnification used due to the low resolution of the method at this magnification.

From the above results, it is clear that the chosen shooting strategy did not bring significant changes in the microstructure of both analysed materials. One reason is probably the large coarseness of the grains of the analysed materials. Therefore, part of the follow-up experiments will deal with the optimization of the materials used and shooting parameters. The second part of the experiments will then deal with a more detailed description of the microstructure of existing samples at higher magnifications and use other metallographic methods such as TEM observation and local EBSD analyses.

This study was supported by the project SGS-2021-030 "Development of new materials, application of modern methods of their processing, ecological production, welding, and testing".

References

1. Kaufman, J., Špirit, Z., Vasudevan, V., Steiner, M., Mannava, S., Brajer, J., Pína, L. and Mocek, T., 2021. Effect of Laser Shock Peening Parameters on Residual Stresses and Corrosion Fatigue of AA5083. Metals, 11(10), p.1635.
2. Špirit, Z., Brajer, J., Kaufman, J., Chocholoušek, M., Bohm, M., Kott, J. and Strejcius, J., 2018. Effect of Laser Shock Peening on Fatigue life of Austenitic stainless steels. IOP Conference Series: Materials Science and Engineering, 461, p.012084.A. Mecke, I. Lee, J.R. Baker jr., M.M. Banaszak Holl, B.G. Orr, Eur. Phys. J. E **14**, 7 (2004)
3. R, S., P, G., Gupta, R., G, R., Pant, B., Kain, V., K, R., Kaul, R. and Bindra, K., 2019. Laser Shock Peening and its Applications: A Review. Lasers in Manufacturing and Materials Processing, 6(4), pp.424-463.

4. Spirit, Z., Kaufman, J., Strejcius, J., Chocolousek, M. and Kott, J., 2019. Increase of the Fatigue Life of Stainless Steel by Laser Shock Peening. DAAAM Proceedings, pp.0826-0831
5. Gujba, A. and Medraj, M., 2014. Laser Peening Process and Its Impact on Materials Properties in Comparison with Shot Peening and Ultrasonic Impact Peening. Materials, 7(12), pp.7925-7974
6. Montross, C., 2002. Laser shock processing and its effects on microstructure and properties of metal alloys: a review. International Journal of Fatigue, 24(10), pp.1021-1036
7. Qiao, H., Zhao, J. and Gao, Y., 2015. Experimental investigation of laser peening on TiAl alloy microstructure and properties. Chinese Journal of Aeronautics, 28(2), pp.609-616
8. Hu, Y., Yao, Z. and Hu, J., 2006. 3-D FEM simulation of laser shock processing. Surface and Coatings Technology, 201(3-4), pp.1426-1435
9. Keller, S., Chupakhin, S., Staron, P., Maawad, E., Kashaev, N. and Klusemann, B., 2018. Experimental and numerical investigation of residual stresses in laser shock peened AA2198. Journal of Materials Processing Technology, 255, pp.294-307
10. Zhou, L., He, W., Luo, S., Long, C., Wang, C., Nie, X., He, G., Shen, X. and Li, Y., 2016. Laser shock peening induced surface nanocrystallization and martensite transformation in austenitic stainless steel. Journal of Alloys and Compounds, 655, pp.66-70
11. Wang, Z., Sun, G., Lu, Y., Chen, M., Bi, K. and Ni, Z., 2020. Microstructural characterization and mechanical behavior of ultrasonic impact peened and laser shock peened AISI 316L stainless steel. Surface and Coatings Technology, 385, p.125403
12. Wang, C., Luo, K., Wang, J. and Lu, J., 2022. Carbide-facilitated nanocrystallization of martensitic laths and carbide deformation in AISI 420 stainless steel during laser shock peening. International Journal of Plasticity, 150, p.103191
13. Wang, C., Luo, K., Bu, X., Su, Y., Cai, J., Zhang, Q. and Lu, J., 2020. Laser shock peening-induced surface gradient stress distribution and extension mechanism in corrosion fatigue life of AISI 420 stainless steel. Corrosion Science, 177, p.109027